

EVOLUTION OF A VOID AND AN ADJACENT GALAXY SUPERCLUSTER IN THE QUASISPHERICAL SZEKERES MODEL

Krzysztof Bolejko

*Nicolaus Copernicus Astronomical Center, Polish Academy of Sciences,
ul. Bartycka 18, 00-716 Warsaw, Poland
bolejko@camk.edu.pl*

This paper investigates the evolution of a void and an adjacent galaxy supercluster. For this purpose the quasispherical Szekeres model is employed. The Szekeres model is an exact solution of the Einstein field equations. In this way investigations of the evolution of the cosmic structures presented here can be freed from such assumptions as small amplitude of the density contrast. Studying the evolution of a void and an adjacent supercluster results not only in better understanding the evolution of cosmic structures but also in acquainting us with the Szekeres model. The main results include the conclusion that small voids surrounded by large overdensities evolve slower than large, isolated voids do. On the other hand, large voids enhance the evolution of adjacent superclusters which evolve much faster than isolated galaxy superclusters.

Keywords: Cosmology; Structure formation; Szekeres model

1. Introduction

The structures which can be observed in the local Universe include small voids among compact clusters, superclusters and large voids surrounded by large walls or long filaments. The present day density contrast of overdense regions is larger than 1¹ and inside voids it descends to -1.² To describe these structures, an exact solution of the Einstein field equations must be employed. However, among the known exact solutions none is flexible enough to describe such complicated structure as our Universe. Therefore, the analysis of this paper will focus on smaller scales. The structures on small scales, up to Mpc can be described by the Szekeres model which is an exact solution of the Einstein field equations.

The structure of this paper is as follows: Sec. 2 presents the Szekeres model; Sec. 3 presents the evolution of pairs void–supercluster in the quasispherical Szekeres model; Sec. 4 presents the role of expansion in the process of structure formation.

2. The Szekeres model

For our purpose it is convenient to use a coordinate system different from that in which Szekeres³ originally found his solution. The metric is of the following form:⁴

$$ds^2 = c^2 dt^2 - \frac{(\Phi' - \Phi \frac{E'}{E})^2}{(\varepsilon - k)} dr^2 - \Phi^2 \frac{(dp^2 + dq^2)}{E^2}, \quad (1)$$

where $' \equiv \partial/\partial r$, $\varepsilon = \pm 1, 0$ and $k = k(r) \leq \varepsilon$ is an arbitrary function of r .

The function E is given by:

$$E(r, p, q) = \frac{1}{2S}(p^2 + q^2) - \frac{P}{S}p - \frac{Q}{S}q + C, \quad (2)$$

2

where the functions $S = S(r)$, $P = P(r)$, $Q = Q(r)$, and $C = C(r)$ satisfy the relation:

$$C = \frac{P^2}{2S} + \frac{Q^2}{2S} + \frac{S}{2}\varepsilon, \quad \varepsilon = 0, \pm 1, \quad (3)$$

but are otherwise arbitrary.

The quasispherical Szekeres model is the case of $\varepsilon = 1$. As was shown in Ref. 5, surface of $t = \text{const}$ and $r = \text{const}$ has a topology of a sphere. However, as S, P and Q are now functions of r , the spheres are not concentric. For the spheres to be concentric, the functions S, P and Q must be constant. Such conditions entail spherical symmetry, with which the Szekeres model becomes the the Lemaitre–Tolman model.^{9,10}

Substituting the metric (1) in the Einstein equations, and assuming the energy momentum tensor for a dust, the Einstein equations reduce to the following two:

$$\frac{1}{c^2}\dot{\Phi}^2(t, r) = \frac{2M(r)}{\Phi(t, r)} - k(r) + \frac{1}{3}\Lambda\Phi^2(t, r), \quad (4)$$

$$4\pi\frac{G}{c^2}\rho(t, r, p, q) = \frac{M'(r) - 3M(r)E'(r, p, q)/E(r, p, q)}{\Phi^2(t, r)[\Phi'(t, r) - \Phi(t, r)E'(r, p, q)/E(r, p, q)]}. \quad (5)$$

Equation (4) can be integrated:

$$\int_0^\Phi \frac{d\tilde{\Phi}}{\sqrt{\frac{2M(r)}{\tilde{\Phi}} - k(r) + \frac{1}{3}\Lambda\tilde{\Phi}^2}} = c[t - t_B(r)]. \quad (6)$$

As can be seen the Szekeres model is specified by 6 functions: $M(r), k(r), t_B(r), S(r), Q(r), P(r)$. However, by a choice of the coordinates, the number of independent functions can be reduced to 5.

The equations of motion $T^{\alpha\beta}_{;\beta} = 0$ are reduced to the continuity equation:

$$\dot{\rho} + \rho\Theta = 0, \quad (7)$$

where Θ is the scalar of expansion and is equal to:

$$\Theta(t, r, p, q) = 3\frac{\dot{\Phi}(t, r)}{\Phi(t, r)} + \frac{\Phi'(t, r) - \dot{\Phi}(t, r)\Phi'(t, r)/\Phi(t, r)}{\Phi'(t, r) - \Phi(t, r)E'(r, p, q)/E(r, p, q)}. \quad (8)$$

In the expanding Universe Θ is positive so the density decreases. The structures which exist in the Universe, emerged either due to slower expansion of the space (formation of overdense regions) or due to faster expansion (formation of underdense regions). In the Friedmann limit $R \rightarrow ra$, where a is the scale factor and $\Theta \rightarrow 3H_0$.

The Szekeres model is known to have no symmetry.⁶ It is of great flexibility and wide application in cosmology⁷ and in astrophysics,^{4,5} and still it can be used as a model of many astronomical phenomena. In this paper it will be employed to study the evolution of cosmic structures in different environments.

2.1. Density contrast

To compare the evolution of different models the change in their density contrast will be considered. Two different types of density contrast indicators are taken into account. The first one is the usual density contrast, $\delta = \rho/\rho_b - 1$, the second one is the spatially invariant density contrast:⁸

$$S_{IK} = \int_{\Sigma} \left| \frac{h^{\alpha\beta}}{\rho^I} \frac{\partial \rho}{\partial x^\alpha} \frac{\partial \rho}{\partial x^\beta} \right|^K dV, \quad (9)$$

where $I \in \mathbb{R}$, and $K \in \mathbb{R} \setminus \{0\}$. This family of the density contrast indicators can be considered as local or global depending on the size of Σ . Such a quantity not only describes the change of density but also the change of gradients and the volume of a perturbed region. So this density indicator describes the evolution of the whole region in a more sophisticated way than the δ . Here only the case $I = 2, K = 1/2$ will be considered.

2.2. Model set-up

To specify the model 5 functions of the radial coordinate need to be known. Let us define the radial coordinate as a value of Φ at the initial instant $t_0 = 0.5$ My after the big bang, i.e., $r := \Phi(r, t_0)$.

Two of these functions will be $t_B(r)$ and $M(r)$. Let us write the mass function in the following form:

$$M(r) = M_0(r) + \delta M(r), \quad (10)$$

where M_0 is the mass distribution as in the homogeneous universe, and δM is a mass correction, which can be either positive or negative. The δM is defined similarly as in the spherically symmetric case:

$$\delta M(r) = 4\pi \frac{G}{c^2} \int_0^r d\tilde{r} R(\tilde{r}, t_0)^2 R'(\tilde{r}, t_0) \delta \bar{\rho}(\tilde{r}), \quad (11)$$

where $\delta \bar{\rho}(r)$ is an arbitrary function chosen to specify the δM . Although $\delta \bar{\rho}(r)$ is not the initial function of density fluctuations (since an initial density fluctuation is a function of all coordinates) it gives some estimation on the initial density fluctuation of the monopole density component.

The next three functions are $P(r), Q(r), S(r)$. All functions defining the model are presented in Table 1. The numerical algorithm used to solve the Szekeres model's equations is presented in detail in Ref. 11.

The chosen background model is the homogeneous Friedmann model with the density:

$$\rho_b = \Omega_m \times \rho_{cr} = 0.24 \times \frac{3H_0^2}{8\pi G}. \quad (12)$$

where the Hubble constant is $H_0 = 74 \text{ km s}^{-1} \text{ Mpc}^{-1}$. The cosmological constant, Λ , corresponds to $\Omega_\Lambda = 0.76$, where $\Omega_\Lambda = (1/3)(c^2\Lambda/H_0^2)$.

3. Models of a void and an adjacent galaxy supercluster

In this section the evolution a void with an adjoining galaxy supercluster is investigated. Although within the Szekeres model more than two structures can be described, such investigations of less complex cases are useful because they enable us to draw some general conclusions without going into too much detail, which could easily obscure the larger picture.

3.1. Models with $P' = 0 = S', Q' \neq 0$

As mentioned above, if $P' = 0 = S' = Q'$ the Szekeres model becomes the Lemaitre–Tolman model. Hence, the class of models considered in this subsection is the simplest generalisation of the spherically symmetric models.

The double structure of a void and adjoining supercluster can be described in the Szekeres model in two different ways. The first alternative is when $\delta M < 0$, the second when $\delta M > 0$. Both these possibilities are examined here.

3.1.1. Model specification

The exact form of the functions used to define models 1 and 2 is presented in Table 1. The density distributions of models 1 and 2 are presented in Fig. 1. As can be seen the model with $\delta M < 0$ has the void in the center, and the adjacent supercluster has an elongated shape. It is the opposite in model 2. The overdense region at the origin is more compact than in model 1, and the adjacent element is the void.

Table 1. The exact form of the functions used to define models 1–4.

Model	t_B	$\delta\bar{\rho}$	S	P	Q
1	0	$-5A \times \exp[-(\ell/8)^2]$	1	0	$b \ln(1 + \ell) \times \exp(-3A\ell)$
2	0	$1.14A \times \exp[-(\ell/9)^2]$	1	0	$c \ln(1 + 0.2\ell) \times \exp(-3A\ell)$
3	0	$-5A \times \exp[-(\ell/8)^2]$	$-\ell^{0.4}$	$0.55\ell^{0.4}$	$0.33\ell^{0.4}$
4	0	$1.14A \times \exp[-(\ell/9)^2]$	$-\ell^{0.9}$	$0.55\ell^{0.8}$	$0.33\ell^{0.8}$

Note: $\ell = r/\text{Kpc}$, $A = 10^{-3}$, $b = -0.6$, $c = 1.45$.

3.1.2. Evolution

In this section we compare the evolution of the density contrast, $\delta(t, r, \theta, \phi)$, and the $S_{2,1/2}(t, \Sigma)$ density indicator for models 1, 2, with the corresponding models of a single void and the models of a single supercluster obtained within the Lemaitre–Tolman model. The Lemaitre–Tolman model is considered because within

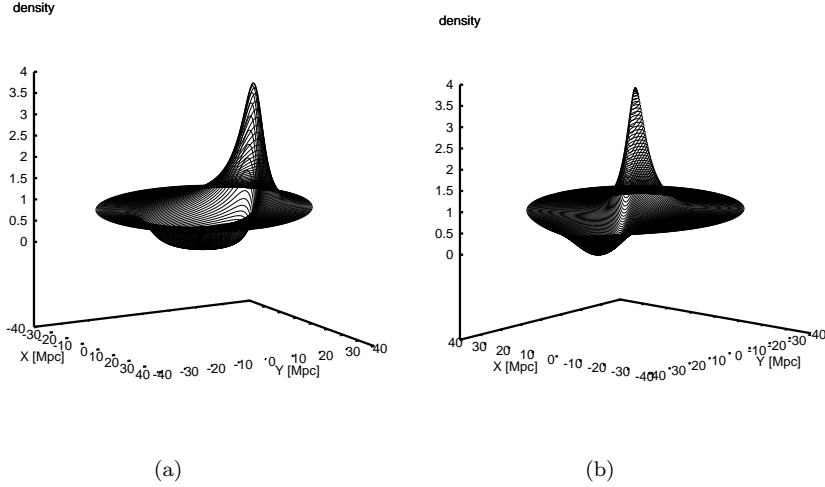


Fig. 1. The present-day density distribution, ρ/ρ_b . Fig. 1(a) presents model 1 ($\delta M < 0$). Fig. 1(b) presents model 2 ($\delta M > 0$).

this model one can describe a single spherically symmetric structure. Such a comparison can demonstrate how the evolution of a structure changes if there is another structure in its close neighbourhood.

Fig. 2 presents the evolution of the density contrast of model 1 in comparison with the corresponding models obtained within the Lemaître–Tolman model. The Lemaître–Tolman model was specified by assuming the same condition as the ones in the Szekeres model at the initial instant. The local density contrast, δ , is compared at the point of the maximal and minimal density value. Fig. 2(a) presents the evolution of the density contrast inside the void. As can be seen the behaviour of the density contrast in both models is similar. This due to the conditions of regularity at the origin (for a detailed description of the regularity conditions at the origin see Ref. 4). These conditions imply that the origin in the quasispherical Szekeres and Lemaître–Tolman model behaves like a Friedmann models Fig. 2(b) presents the evolution of the density contrast at the very center of the overdense region of the model 1 and the corresponding Lemaître–Tolman model. The growth of density contrast in the Szekeres model is much faster than in the corresponding Lemaître–Tolman model. The results of this comparison indicate that within the perturbed region of mass below the background mass ($\delta M < 0$) the evolution of underdensities does not change but the evolution of the overdense regions situated at the edge of the underdense regions is much faster than the similar evolution of isolated structures.

The evolution of the density contrast of model 2 ($\delta M > 0$) is presented in Fig. 3, the evolution of the density contrast at the point of minimal density is depicted in Fig. 3(a), and the evolution at the origin is depicted in Fig. 3(b). Similarly as in model 1, the evolution at the origin in the Szekeres model and in the Lemaître–Tolman model are very much alike. The evolution of the void, however, is slower

within the Szekeres model than it is in the Lemaître–Tolman model. This implies that single, isolated voids evolve much faster than the ones which are in the neighborhood of large overdensities where the mass of the perturbed region is above the background mass ($\delta M > 0$).

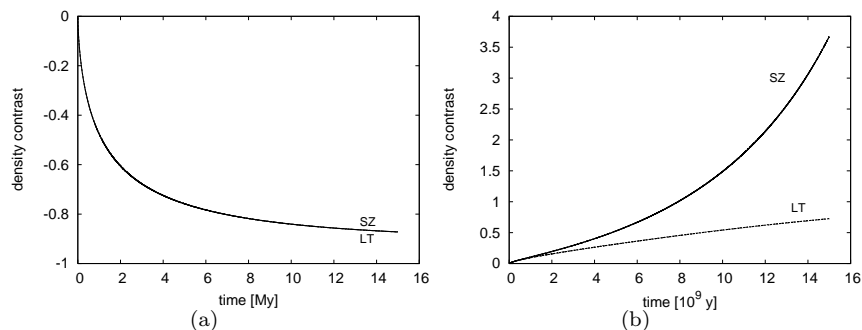


Fig. 2. The evolution of the density contrast inside the void (a), and inside the supercluster (b) for model 1 ($\delta M < 0$). The curve SZ presents the evolution within the Szekeres model; curve LT presents the evolution within the Lemaître–Tolman model.

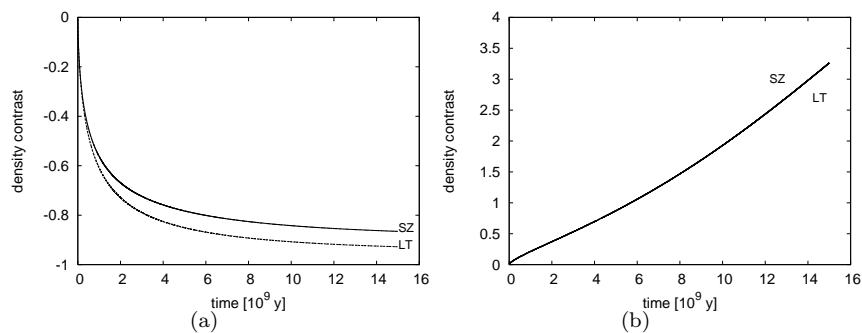


Fig. 3. The evolution of the density contrast inside the void (a), and inside the supercluster (b) for model 2 ($\delta M > 0$). The curve SZ presents the evolution within the Szekeres model; curve LT presents the evolution within the Lemaître–Tolman model.

3.2. Models with $P' \neq 0 \neq S'$, $Q' \neq 0$

In this section models of non-constant P, Q and S are investigated. The evolution of these models is compared with the evolution of models which were considered in Sec. 3.1

3.2.1. Models specification

The exact form of the functions used to define models 3 and 4 is presented in Table 1. Fig. 4 presents the comparison of the present day density distribution in models 1 and 3 in colour coded diagrams. It presents the vertical cross-sections of the considered structures. Fig. 4(a) presents the vertical cross-section through the surface of $\phi = \pi/2$ and Fig. 4(b) presents the cross section through the surface of $\phi \approx \pi/6$. The comprehensive study of the vertical and horizontal cross-sections of similar models was presented in Ref. 12. Fig. 5 also presents the vertical cross-sections of models 2 and 4. As can be seen, both structures appear to be similar but, in comparison with model 1, in model 3 the additional component is moved down and right. Model 4 on the other hand presents the structure moved down and right in comparison with model 2.

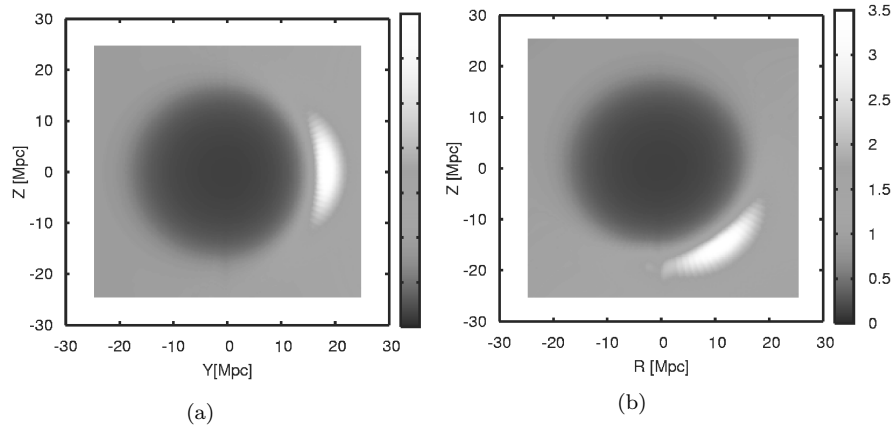


Fig. 4. The present-day colour coded density distribution, ρ/ρ_b , of models with $\delta M < 0$. (a) presents the model with $P' = S' = 0$. (b) presents the model with $P' \neq 0 \neq S'$.

3.2.2. Evolution

The evolutions of the density contrast inside the voids and superclusters of models 3 and 1 are very similar which needn't be surprising as model 3 has the same $\bar{\delta}(r)$ as model 1. Also, the evolutions of the corresponding density contrasts of model 4 and 2 are similar. The functions S, P, Q were chosen so they reproduce the same shape of current structures and the same density contrast inside them — that is why the evolution of a local density contrast is comparable for models 1 and 3, and for models 2 and 4. However, it is not clear whether or not the evolution of $S_{2,1/2}$ is comparable too. When the functions S, P, Q are not constant, the axis of a density dipole changes. Also, the volume of the perturbed region as well as the density gradients can be different. So it may be interesting to compare the evolution

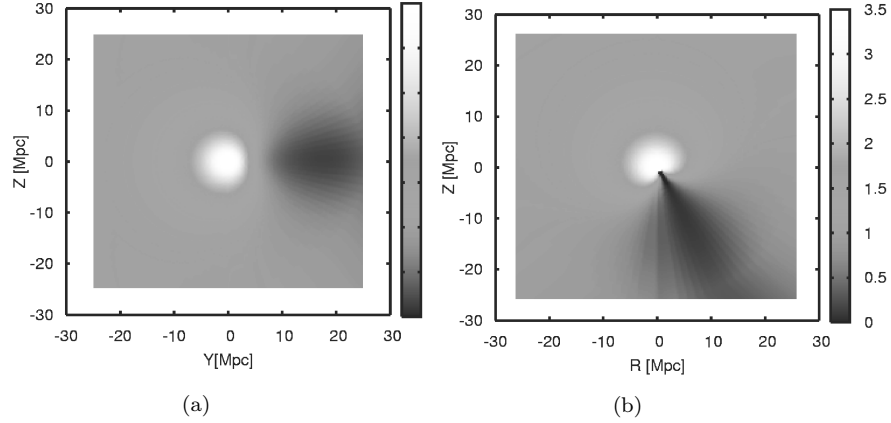


Fig. 5. The present-day colour coded density distribution, ρ/ρ_b , of models with $\delta M > 0$. (a) model with $P' = S' = 0$. (b) model with $P' \neq 0 \neq S'$.

of the whole perturbed underdense and overdense regions of models 1, 2, 3, and 4.

Fig. 6 presents the comparison of evolution of $S_{2,1/2}$ for models 1–4. The primed letters denote models of $S' \neq 0 \neq P', Q' \neq 0$. As can be seen the evolution of $S_{2,1/2}$ for all these models is also comparable. These results imply that the evolution in the quasispherical Szekeres model does not depend on the position of the dipole component. As long as the shape and density contrast of the analysed models are similar, such models evolve in a very similar way.

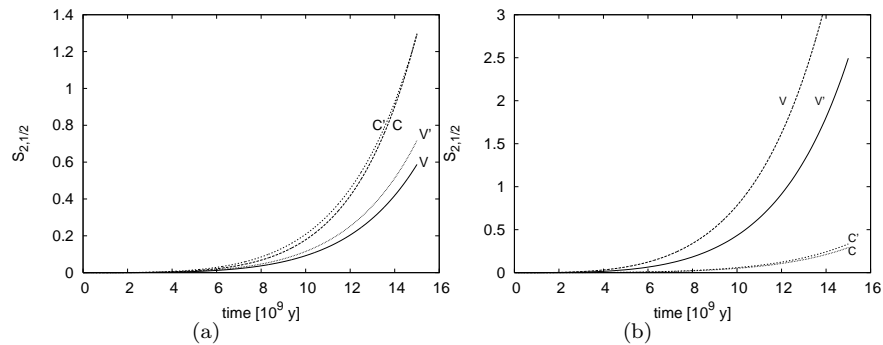


Fig. 6. Comparison of $S_{2,1/2}$ for models with $\delta M < 0$ (a) and with $\delta M < 0$ (b). C corresponds to a "supercluster" — an overdense region, and V corresponds to a "void" — underdense region. Primes denote models with $P' \neq 0 \neq S'$. Since the value of S_{IK} depends on units, the results presented here were normalised so they are now of order of unity.

4. The role of expansion

The faster or slower evolution rate of the previously presented models is reflected by their current expansion rate. As has been shown above, the evolution does not depend on a relative position of the dipole component (evolution of models 1 and 3 is similar). Thus, let us focus on model 1 and model 2 only.

Fig. 7 presents the ratio, Θ_{SZ}/Θ_0 , of the expansion parameter in the considered Szekeres models to the expansion parameter in the homogeneous background. As can be seen, model 1, with $\delta M < 0$, has a larger amplitude of this ratio, and the evolution of a supercluster in this model is much faster than in the corresponding Lemaître–Tolman model. On the other hand, model 2 ($\delta M > 0$) has smaller amplitude of the Θ_{SZ}/Θ_0 ratio and within model 2 the evolution of the density contrast inside the void was much slower than in the Lemaître–Tolman model. So clearly the rate of the evolution is connected with the rate of the expansion. This conclusion is also supported by the continuity equation [Eq. (7)]. Higher mass in the perturbed region slows down the expansion rate — this is a condition hindering the evolution of cosmic voids. On the other hand, if the mass of perturbed region is below the background mass, such region expands much faster than the background, leading to the formation of the large underdense regions. Such large voids enhance the formation of large elongated overdensities (walls) formed at the edges of voids.

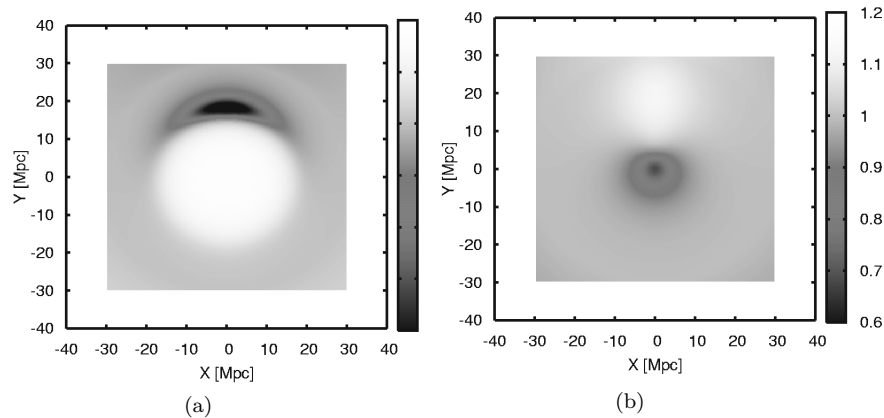


Fig. 7. The Θ_{SZ}/Θ_0 ratio. (a) presents the ratio of model 1. (b) presents the ratio of model 2.

5. Conclusions

The galaxy redshift surveys show that the Universe is patchy with various structures. These structures include small voids among compact superclusters and large voids surrounded by large walls or long filaments.

The evolution of these cosmic structures in different environments in the quasi-

spherical Szekeres model was investigated. The Szekeres model is the most complex spatially inhomogeneous exact solutions of the Einstein field equations, and it is of great use in cosmology. Since it is an exact solution of Einstein's equations, it enables us to investigate the evolution of cosmic structures without such approximations as linearity and small amplitude of density contrast. Moreover, the Szekeres model is flexible enough to describe more than one structure.

Having investigated various models with two or three structures within one frame it may be concluded that the evolution of the cosmic structures depends on the environment. In perturbed a region whose mass is below the background mass the amplitude of the expansion's fluctuations is large and as can be seen from the continuity equation [Eq. (7)], such conditions enhance the evolution of cosmic structures.

The analyses presented in this paper indicate that small voids among large overdense regions do not evolve as fast as the large voids do. This is because the expansion of the space is faster inside large voids than inside smaller voids. Moreover, this higher expansion rate inside the large voids leads to the formation of large and elongated structures such as walls and filaments which emerge at the edges of these large voids.

Acknowledgments

I would like to thank Andrzej Krasinski and Charles Hellaby for their valuable comments and discussions concerning the Szekeres model.

References

1. E. Branchini, et al., *Mon. Not. R. Astron. Soc.* **308**, 1 (1999).
2. F. Hoyle and M. S. Vogeley, *Astrophys. J.* **607**, 751 (2004).
3. P. Szekeres, *Commun. Math. Phys.* **41**, 55 (1975).
4. C. Hellaby and A. Krasinski, *Phys.Rev. D* **66**, 084011 (2002).
5. P. Szekeres, *Phys. Rev. D* **12**, 2941 (1975).
6. W. B. Bonnor, A. H. Sulaiman, and N. Tomimura, *Gen. Relativ. Gravit.* **8**, 549 (1977).
7. W. B. Bonnor and N. Tomimura, *Mon. Not. R. Astron. Soc.* **175**, 85 (1976).
8. F. Mena and R. Tavakol, *Class. Quant. Grav.* **16**, 435 (1999).
9. G. Lemaitre, *Ann. Soc. Sci. Bruxelles* **A53**, 51 (1933); reprinted in *Gen. Relativ. Gravit.* **29**, 641 (1997).
10. R. C. Tolman, *Proc. Nat. Acad. Sci. USA* **20**, 169 (1934); reprinted in *Gen. Relativ. Gravit.* **29**, 935 (1997).
11. K. Bolejko K., in *13th Young Scientists' Conference on Astronomy and Space Physic*, eds. A. Golovin, G. Ivashchenko and A. Simon, (Kiev University Press, 2006); astro-ph/0607130.
12. K. Bolejko K., *Phys. Rev. D* **73**, 123508 (2006).